

Solvent Induced Polymorphism in Supramolecular 1,3,5-Benzenetribenzoic Acid Monolayers

Lorenz Kampschulte,[†] Markus Lackinger,^{*,†,‡} Anne-Kathrin Maier,[†] Ravuri S. K. Kishore,[§] Stefan Griessl,[†] Michael Schmittl,[§] and Wolfgang M. Heckl^{†,‡,¶}

Department für Geo- und Umweltwissenschaften, Ludwig Maximilians Universität München and Center for Nanoscience (CeNS), Theresienstrasse 41, D-80333 München, Germany, Department of Physics and Astronomy, University of California Irvine, Frederick Reines Hall, Irvine, California 92697-4575, Center of Micro and Nanochemistry and Engineering, Organische Chemie I, Universität Siegen, Adolf-Reichwein-Strasse 2, D-57068 Siegen, Germany, and Deutsches Museum, Museumsinsel 1, D-80538 München, Germany

Received: December 28, 2005; In Final Form: March 18, 2006

This work presents a scanning tunneling microscopy (STM) based study of benzenetribenzoic acid (BTB) monolayer structures at the liquid–solid interface. On graphite(0001) the tailored molecules self-assemble into 2D supramolecular host systems, suitable for the incorporation of other nanoscopic objects. Two crystallographically different BTB structures were found—both hydrogen bonded networks. A specific structure was deliberately selected by solvent identity. One of the BTB polymorphs is a 6-fold chicken-wire structure with circular, approximately 2.8 nm wide cavities. The other structure exhibits an oblique unit cell and a different hydrogen bonding pattern. The large cavity size of the chicken-wire structure was made possible through comparatively strong 2-fold hydrogen bonds between carboxylic groups. In addition, the low conformational flexibility of BTB was supportive to combat the tendency for dense packing.

Introduction

Due to their high directionality, hydrogen bonds play a key role in molecular recognition processes, in solution, in the solid state and for surface patterning. Two-dimensional hydrogen bonded networks on surfaces demonstrate the unique potential of tailoring supramolecular assemblies for nanotechnology applications. Among others, the carboxylic acid functionality typically exhibits robust hydrogen bonds with itself, with the hydroxyl group acting as a donor and the carbonyl oxygen as an acceptor. In a symmetrical, polyfunctional disposition, the interplay of multiple hydrogen-bonding leads to well organized structures on surfaces and in bulk crystals. For instance, the para-position of the carboxylic groups in terephthalic acid (TPA) results in formation of hydrogen bonded linear chains on a surface.^{1,2} Also, the relative position of functional groups in substituted porphyrin molecules can be exploited to steer the self-assembly process.³ Among hydrogen bonded supramolecular structures, two-dimensional template structures enable ordering^{4,5} and addressing of nanometer sized objects such as clusters^{6–8} or functional molecules^{9,10} on surfaces with sub-nanometer precision. These template structures exhibit a periodic arrangement of cavities of various size and shape, where the guest species can be confined. As has been shown recently, the archetypical supramolecular model system trimesic acid (TMA, cf. Figure 1a) is well suited for this purpose. TMA can be considered a smaller analogue of BTB (cf. Figure 1b), with similar symmetry and the same functional groups for forming hydrogen bonds. Scanning tunneling microscopy (STM) experi-

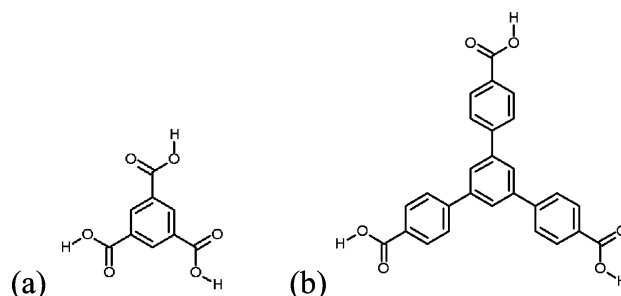


Figure 1. Chemical structures of (a) trimesic acid (TMA, C₉H₆O₆) and its larger analogue (b) 1,3,5-benzenetribenzoic acid (BTB, C₂₇H₁₈O₆)

ments in an UHV environment with evaporated TMA monolayers on graphite(0001) revealed two different polymorphs: chicken-wire and flower structure.¹¹ Both structures are governed by intermolecular hydrogen bonding and exhibit a periodic arrangement of approximately 1.0 nm wide circular cavities. Similarly, a TMA chicken-wire structure was found on Cu(100).¹² However, due to stronger interaction with the metal substrate, the TMA lattice was slightly distorted and no large domains could be grown. Among others, a TMA chicken-wire structure was realized on Au(111) in an electrochemical STM study for suitable potential conditions.¹³ Another EC-STM study of TMA, equally on Au(111) found various densely packed phases with upright molecules and potential driven phase transitions, revealing the influence of a stronger adsorbate–substrate interaction.¹⁴ In addition, a more comprehensive EC-STM study of TMA on Au(111) complemented by ATR SEIRAS (attenuated total reflection surface enhanced infra red adsorption spectroscopy) found phases with upright TMA molecules and coadsorbed interfacial water molecules inhibiting intermolecular hydrogen bonds between TMA molecules.¹⁵ Bai et al. succeeded in growing and characterizing a hexagonal two-dimensional host system, likewise on HOPG (highly oriented pyrolytic graphite)

* Corresponding author. Phone: +49 89 2180 4185. Fax: +49 89 2180 4334. E-mail: markus@lackinger.org.

[†] Ludwig Maximilians Universität München and Center for Nanoscience (CeNS).

[‡] University of California Irvine.

[§] Universität Siegen.

[¶] Deutsches Museum.

with an enlarged cavity diameter of 1.9 nm.¹⁶ This study applied a molecule related to TMA, but with additional C—O—C spacers between the aromatic core and the three carboxylic groups, respectively. In UHV co-deposition experiments, Theobald and co-workers combined PTCDI (perylene tetracarboxylic diimide) and melamine to form a hexagonal hetero-molecular host network with a fairly large lattice constant of 3.46 nm.¹⁷ In this case 3-fold intermolecular hydrogen bonds were the driving force for the self-assembly process and the symmetry of the adlayer was governed by the 3-fold symmetry of melamine. As has been shown in this work, the cavities are large enough to incorporate up to seven C₆₀ fullerene molecules within a single cell. Equally, it was possible to prepare a mixed-network at the liquid–solid interface composed of TMA and TPT (1,3,5-tris-(4-pyridyl)-2,4,6-triazine) through adsorption from binary solutions.¹⁸ Furthermore, it has been demonstrated that in equilibrium with the liquid phase TPT only adsorbs in the presence of a second species, which acts as a linker. Thereby, larger noncovalently bonded aggregates with sufficiently large adsorption energy are generated. The necessity for a linking species arises because TPT by itself provides only a functional group acting as a hydrogen bond acceptor, thereby rendering intermolecular TPT–TPT hydrogen bonds impossible. However, adding TMA or TPA as a linker molecule provided mixed networks bonded over N···H—O hydrogen bonds. Because the size and geometric structure of TPT is comparable to BTB, these results already indicate the crucial role of the carboxylic groups for the stabilization of the discussed interfacial monolayers. Various studies demonstrated that the increased binding strength of metal–organic coordination complexes can be exploited to grow various host-systems.¹⁹ However, up to now this approach seems to be limited to UHV based preparation techniques.

Moreover, it was demonstrated at the liquid–solid interface that a supramolecular TMA host structure, as its primary purpose, can be used for the storage and manipulation of single molecules approximately one nanometer in size.^{20,21} Similarly, it has been shown that copper phthalocyanine as well as coronene are suitable guests in a host network composed of 1,3,5-tris(10-carboxydecyloxy)benzene on HOPG.²² In the latter study a volatile solvent (toluene) was used and in contrast to the results presented herein, the structures were not investigated in equilibrium with the liquid phase above.

Because functional molecules, such as amino acids and small proteins in biology or metal clusters in solid-state physics and molecular electronics, vary in size and shape, deliberate tuning of the cavity dimensions of the host structure is a basic requirement for incorporation of these guests. To generate a two-dimensional homomeric (i.e., composed of one kind of molecule only) host network on a graphite surface with large cavities, we turned our attention to 1,3,5-benzenetribenzoic acid (BTB), a *D*_{3h} symmetric molecular building block (cf. Figure 1b) equipped with three 4-carboxyphenyl arms. BTB is also a popular ingredient for highly porous bulk crystals with large specific surfaces, which often take advantage of metal–organic bonds.²³

A major challenge in the design of host systems is tuning the cavity size and shape in a controlled manner. It is necessary to combat the tendency of the molecular building blocks toward dense packing, instead of crystallization in a structure with large, energetically unfavorable cavities. The principle of closest packing as enunciated by Kitaigorodskii^{24,25} holds for weak interacting building blocks. Thus, increasing the interaction through hydrogen bonds offers a way to circumvent the tendency for close packing.

In STM studies of Bai et al.,²⁶ comparable C₃ symmetric molecules with a benzene ring as a core and three attached alkoxy-carboxylic acid groups as hydrogen bonding sites were used. However, due to the use of flexible aliphatic spacers of variable length, these molecules preferred dense packing on the surface. In contrast, any conformational changes in 1,3,5-benzenetribenzoic acid (BTB), i.e., rotation around the C_{ph}—C_{ph} and the C_{ph}—C_{COOH} bonds, will not change the main directionality of the hydrogen bonding units, i.e., the carboxylic groups. In this work we show that the rigidity of the BTB molecules and the strong intermolecular interaction introduced by hydrogen bonds in combination with a proper solvent result in a periodic adsorbate structure with fairly large cavities. In addition, with various other solvents a more densely packed structure was observed.

Experimental Section

BTB [1,3,5-tris(4-carboxyphenyl)benzene (1,3,5-benzenetribenzoic acid)] was synthesized according to a known literature procedure²⁷ by a tricarboxylation of 1,3,5-tris(*p*-bromophenyl)-benzene. BTB: ¹H NMR (400 MHz, DMSO-*d*₆) δ 8.00 (d, *J* = 8 Hz, 6 H, m-H), 8.29 (d, *J* = 8.03 Hz, 6 H, o-H), 8.05 (s, 3 H, H); ¹³C NMR (100.6 MHz, DMSO-*d*₆) δ 125.6, 127.5, 130.0, 130.1, 140.8, 143.9, 167.3; EI mass (*m/z*) 438 (M⁺); IR (KBr) 3600–2400 (OH), 1680 (C=O), 1600, 1560, 1420 (C=C), 1290 (C—O), 850, 765, 700 (CH) cm^{−1}.

STM measurements at the liquid–solid interface were carried out at room temperature with a home-built STM, driven by a commercial SPM-100 control system from RHK. Submolecularly resolved images were obtained in the constant current mode of operation. Typically, bias voltages of +0.3, ..., +1.5 V with respect to the tip, and current set points of about 0.1, ..., 0.9 nA were applied. For noise reduction, all STM images were processed by leveling and a 3 × 3 G filtering. The following solvents were used for the experiments: butanoic acid (>99%, Fluka), pentanoic acid (>98%, Fluka), hexanoic acid (>98%, Fluka), heptanoic acid (>99%, Sigma Aldrich), octanoic acid (>99%, Sigma Aldrich), nonanoic acid (>97%, Fluka), 1-octanol (>99%, Merck), 1-nonanol (>98%, Merck Schuchardt), 1-decanol (>97%, Merck Schuchardt), 1-phenyloctane (>98%, Merck Schuchardt), dodecane (>98%, Fluka). These solvents are electrically nonconductive and their vapor pressure at room temperature is sufficiently low to allow for stable tunneling experiments in the order of 1 h. Mechanically cut tunneling tips from a Pt/Ir wire (90/10) without any insulation were used.

All samples were prepared by applying a droplet of the respective BTB solution on a freshly cleaved HOPG(0001) surface. The self-assembled interfacial monolayer was characterized by in-situ STM with the tip being immersed in the solution. To precisely measure lattice parameters and determine the superstructure matrices, the graphite lattice and the self-assembled monolayer were imaged within the same frame. In the first part the adsorbate layer was imaged; in the second part the substrate lattice was imaged by decreasing the tunneling voltage and increasing the tunneling current set point. The experimental error in the coefficients of the superstructure matrix is in the range of ±0.5. Although the accuracy does not allow the assignment of a truly commensurate adsorbate lattice, the matrices have been assumed to be commensurate. Even on weak interacting substrates, like layered materials, normally a certain relation between adsorbate and substrate lattice like commensurability or point-on-line structures exist.

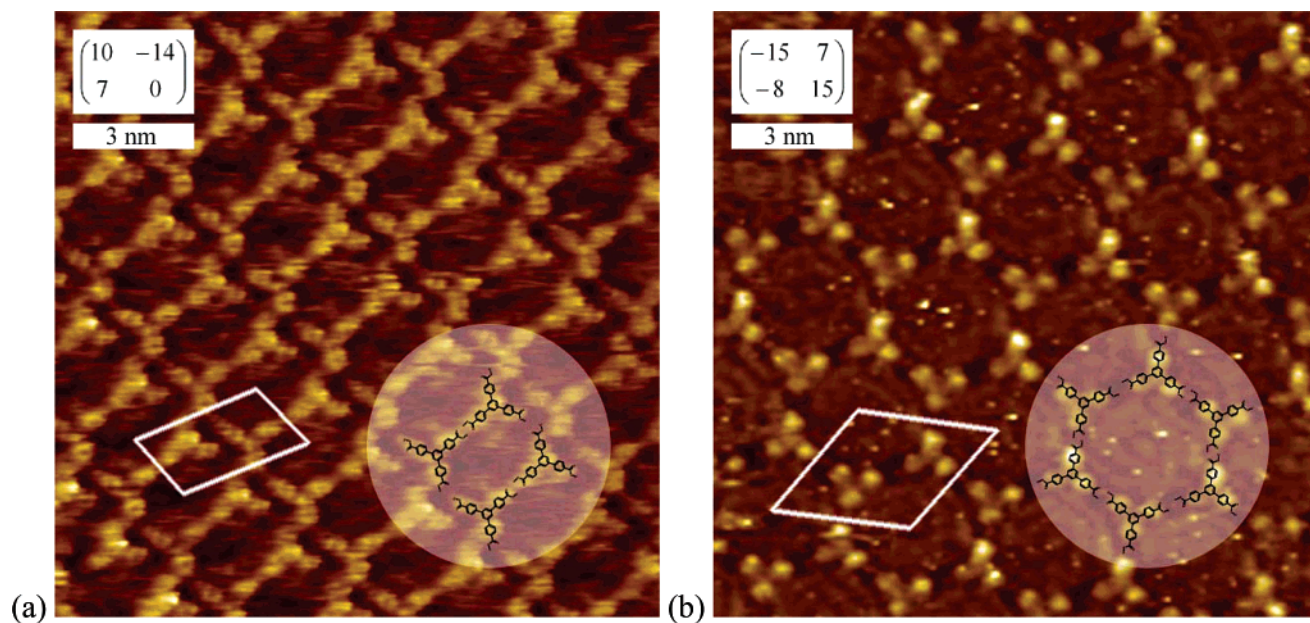


Figure 2. STM topographs of the BTB monolayers, self-assembled on a HOPG(0001) surface. The superstructure matrices (referred to the hexagonal lattice of every second graphite atom—lattice constant 0.246 nm and 60° —as visible in atomically resolved STM images) are given in the insets and the positions of individual BTB molecules are indicated. (a) shows the modification with the oblique unit cell as obtained in butanoic through heptanoic acid, 1-octanol, 1-nonanol, and 1-decanol, and (b) shows the hexagonal chicken-wire modification as obtained in nonanoic acid and 1-phenyloctane. For octanoic acid and dodecane both modifications were observed.

Results and Discussion

For BTB monolayers at the interface between graphite(0001) and saturated solution two different, non-densely-packed polymorphic modifications were revealed as a function of the applied solvent by means of in-situ STM. These two structures differ in their hydrogen bonding pattern and their particular molecular packing density. Dependent on solvent identity either an oblique or a hexagonal unit cell was observed, with the former structure exhibiting rectangular cavities, and the latter circular cavities. Representative STM topographs of both structures are depicted in Figure 2a,b, respectively. The superstructure matrices of the adsorbate lattices with respect to the graphite substrate are given in the insets.

In both structures, single BTB molecules appear with a 3-fold symmetric shape in the STM topographs and their size is consistent with flat lying molecules. Thus, the STM contrast is dominated by the geometry of the molecule.

It has been shown recently that fatty acid solvent molecules can form mixed monolayers with coronene solute molecules on Au(111).²⁸ Thus, solvent coadsorption can have a great impact on both the emerging monolayer structure and the STM contrast within the cavities. In this study, upright fatty acid molecules adsorbed with their carboxylic groups directly to the substrate were proposed and clearly resolved in the STM topographs. But the adsorption energy on Au(111) exceeds that on weakly interacting graphite(0001). Furthermore, deprotonation of the bonding carboxylic group might play a crucial role for their bonding to metal surfaces. In our networks, however, we do not clearly observe the incorporation of solvent molecules in the BTB structures. On the other hand, an internal structure was reproducibly found within the cavities of the chicken-wire structure. For reasons of spacing and symmetry, it can be ruled out that just the underlying graphite substrate is atomically resolved within the cavity. It is, however, most likely that either solvent or additional BTB molecules are loosely bound within the cavities.

Butanoic, pentanoic, hexanoic, and heptanoic acid, 1-octanol, 1-nonanol, and 1-decanol as solvents lead to a BTB surface

structure with an oblique unit cell (indicated in Figure 2a), where four molecules border rectangular cavities. The positions of the molecules within the unit cell as well as the superstructure matrix are given in Figure 2a. The size of the unit cell amounts to $(1.7 \times 3.1) \text{ nm}^2$ with an angle of 76° between the adsorbate lattice vectors and contains two BTB molecules. Evidently, the basic unit of this structure is a BTB dimer motif, where the BTB molecules are rotated 180° with respect to each other and bonded by a 2-fold hydrogen bond between two carboxylic groups. These dimers are aligned along rows with their axis almost perpendicular to the row. However, it is difficult to assign the bonding scheme among those dimers. A tentative model, which is based on the relative position as deduced from the STM images, is depicted in Figure 3a. The bonding pattern proposes four $\text{O}\cdots\text{H}-\text{O}$ hydrogen bonds per BTB dimer within the rows and additional four weaker $\text{O}\cdots\text{H}-\text{C}$ hydrogen bonds per BTB dimer among neighboring rows. According to the scaled model, the distance between the free carbonyls of the acid groups and the H atoms amounts to $\sim 0.29 \text{ nm}$ and thus lies well within the range of $\text{O}\cdots\text{H}-\text{C}$ hydrogen bonds.²⁹ Furthermore, an ab initio calculation concludes that the supposedly weak $\text{O}\cdots\text{H}-\text{C}$ bonds can have a major impact on the structure formation, rather than being a mere consequence of the crystal packing.³⁰ According to this packing, the rows of dimers are shifted with respect to each other.

In general, the packing of BTB or analogous compounds in bulk crystals should give an indication of the nature of the hydrogen bonding that such systems might show affinity for on the graphite–liquid interface. Although there has been no report on the X-ray crystal structure of BTB, systems containing multiple carboxylic acid moieties have been studied.^{31,32} Of specific interest is the hydrogen-bonding behavior in TMA bulk crystals. The most common polymorph of TMA in crystals is the infinite chicken-wire motif arising from the dimer motif, which is observed commonly in 90% of the carboxy containing crystal structures in the Cambridge Structural Database (CSD) analysis.³³ This behavior is consistently carried on to the liquid–solid interface, as has been reported recently.³⁴

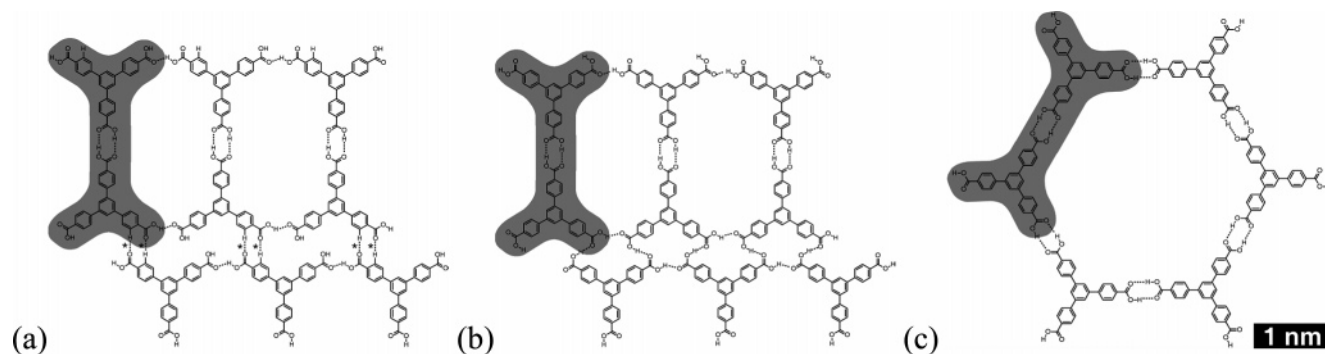


Figure 3. (a) Proposed hydrogen bonding pattern for the oblique BTB polymorph. Dimers in the same row are bonded by a total of four $\text{O}\cdots\text{H}-\text{O}$ hydrogen bonds to their neighboring dimers. Between the rows the BTB dimers are bonded by weak $\text{O}\cdots\text{H}-\text{C}$ hydrogen bonds only (marked by asterisks). To establish those bonds, the rows are shifted with respect to each other by approximately half the dimer-dimer distance. (b) An alternative model for the oblique BTB polymorph based on syn-anti-syn catemer hydrogen bonding between the dimer rows. Similar to (a), the dimer rows are shifted with respect to each other. (c) Proposed hydrogen bonding pattern of the BTB chicken-wire polymorph solely based on the dimer motif. Every carboxylic group forms a 2-fold straight hydrogen bond with an adjacent carboxylic group, resulting in a total of six hydrogen bonds per BTB molecule.

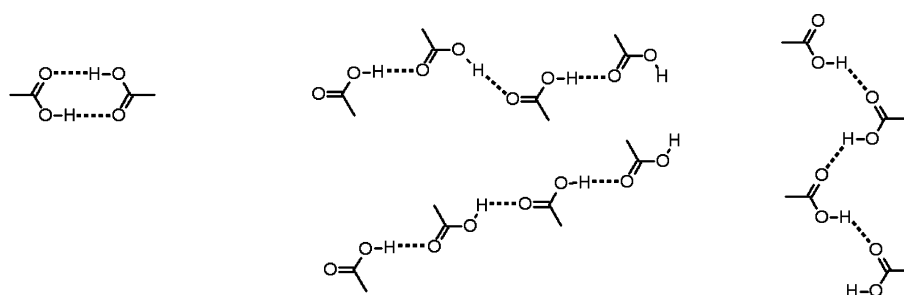


Figure 4. Observed hydrogen bonding patterns in organic crystals of carboxy containing compounds: left-hand side, dimer motif with a 2-fold hydrogen bond; center and right-hand side, various catemer motifs depending on the syn and anti conformation of the constituent carboxylic acid.

However, there exist other hydrogen bonding patterns in carboxylic acid crystal structures apart from the dimer, namely the catemer motifs, which account for the remaining 10% of the crystal structures in the CSD.³³ Three different catemer motifs are known to exist depending on the syn and anti conformation of the constituent carboxylic acid groups.³¹ Figure 4 provides an overview about the dimer and the various catemer hydrogen bonding patterns among carboxylic groups.


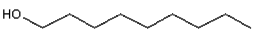

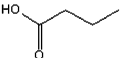
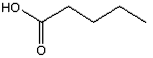
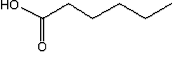
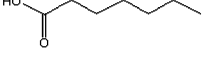
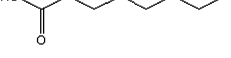

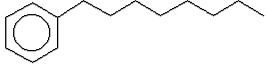

Based on the catemer hydrogen bonding pattern, an alternative model for the rectangular BTB polymorph is equally conceivable and depicted in Figure 3b. Both the $\text{O}\cdots\text{H}-\text{C}$ hydrogen bond stabilized structure and the syn-anti-syn catemer pattern are in accordance with the 2D crystallographic data as obtained by STM. Based on the 2D pattern only, it is not possible to predict which of the above patterns is followed, yet total energy calculations might provide deeper insight. Nevertheless, the materialization of a lower symmetry structure in the self-assembly process implies the evolution of alternative hydrogen bonding patterns besides the dimer motif. Deviations from the ideal dimer motif in the hydrogen bonded monolayer structures have been observed in various other systems.^{34,35}

The second BTB structure as observed in nonanoic acid and 1-phenyloctane, consists of hexagonally arranged and interconnected six-membered rings. Basically, those rings are composed of three BTB dimers each. Every possible hydrogen bond between the three carboxylic groups of BTB is formed under an energetically ideal bonding angle of 180° . This results in a total of six hydrogen bonds (two for each two adjacent carboxylic groups) per molecule. Each BTB molecule is part of three adjacent rings. A model of the structure is given within the STM image in Figure 2b and in Figure 3c. The circular cavities have a diameter of about 2.8 nm. Similar to the oblique structure, the basic unit is a dimer motif.

It is noteworthy that, by using octanoic acid as a solvent—the size and molecular weight of which lies between heptanoic and nonanoic acid—both polymorphic modifications can be found coexisting on the surface. The coexistence of both monolayer structures has also been observed in dodecane. During the experimental time span, which is limited by evaporation of the solvent, no transformations of one phase into the other was observed. Thus, a conclusion of which phase is thermodynamically more stable cannot be drawn.

The effect of solvent induced polymorphism is well-known from organic bulk crystals and of great importance, for example, in the pharmaceutical industry, because different modifications usually differ in their physical properties. Similarly, in a previous study we found different monolayer polymorphs for TMA depending on the solvent at the liquid–solid interface.³⁴ Both TMA and BTB form a related chicken-wire structure, which is identical in symmetry and the hydrogen bonding pattern but differs by a factor of ~ 1.9 in lattice constant. However, the respective second polymorphic modification is not related at all. Only the respective chicken-wire polymorph exhibits the energetically ideal, straight 2-fold hydrogen bond between adjacent carboxylic groups, whereas, in the so-called TMA flower structure one-third of all hydrogen bonds participate in a circular scheme with three carboxylic groups of three TMA molecules involved. Another comparable circular arrangement of hydrogen bonds has been proposed by Bai and co-workers for tetrakis(carboxylphenyl)porphyrin monolayers on graphite.³⁵ For TMA as well as for BTB, the denser structure was found for fatty acids with shorter chain length: In the case of BTB values of 0.39 molecules/ nm^2 for the oblique structure vs 0.23 molecules/ nm^2 for the chicken-wire polymorph were found; lattice parameters of all respective TMA and BTB structures are listed in Table 2. Of course, the difference in the absolute

TABLE 1: Solvents Applied in This Study and the Resulting BTB Monolayer Structure on the Solvent–HOPG Interface^a

no.	solvent	chemical structure	functional group	ϵ (temp. (K))	monolayer structure
1	1-octanol		R-OH	10.30 (293.2) ³⁶	oblique
2	1-nonanol		R-OH	8.83 (293.2) ³⁶	oblique
3	1-decanol		R-OH	7.93 (293.2) ³⁶	oblique
4	butanoic acid		R-COOH	3.02 (303.2) ³⁷	oblique
5	pentanoic acid		R-COOH	2.93 (303.2) ³⁷	oblique
6	hexanoic acid		R-COOH	2.61 (303.2) ³⁷	oblique
7	heptanoic acid		R-COOH	3.04 (303.2) ³⁷	oblique
8	octanoic acid		R-COOH	2.82 (303.2) ³⁷	oblique + hexagonal
9	nonanoic acid		R-COOH	2.50 (302.8) ³⁷	hexagonal
10	1-phenyloctane		R-(aromatic)	2.26 (293.2) ³⁶	hexagonal
11	dodecane		R	2.01 (293.2) ³⁶	oblique + hexagonal

^a The temperature dependence of the dielectric constants in the range room temperature ± 10 K is insignificant.³⁷

TABLE 2: Unit Cell Parameters and Molecular Area Densities of the Two BTB and TMA Polymorphic Structures

structure	unit cell parameters			area density (1/nm ²)	relative area density (%)	
	<i>a</i> (nm)	<i>b</i> (nm)	α (deg)		molecules	cavity
BTB oblique	1.7	3.1	76	0.39	66	34
BTB chicken-wire	3.2	3.2	60	0.23	38	62
TMA flower	2.5	2.5	60	1.11	84	16
TMA chicken-wire	1.7	1.7	60	0.80	61	39

values in comparison to those for TMA is because of the larger size of BTB. In addition, based on these molecular densities, the relative area of the cavity, where the pristine substrate is exposed to the liquid phase has been calculated for all BTB and TMA structures. The projection of the van der Waals surface perpendicular to the molecular plane was used as molecular area, resulting in 1.69 nm² for a BTB and 0.76 nm² for a TMA molecule.

As stated above, a common feature of the self-assembly of TMA and BTB monolayers at the liquid–solid interface is the chicken-wire polymorph emerges for fatty acid solvents with longer aliphatic tail. The general trend of seeing a higher symmetrical arrangement (chicken-wire) of the TMA and BTB molecules on the substrate by using these solvents can readily be explained by invoking the principle of polarity. The dielectric constant ϵ (cf. Table 1) decreases along the homologous series from butanoic acid (3.02) to nonanoic acid (2.50) and is known to play a strong role in dictating the properties of alkanolic acids.^{38,39} For example, the association constants of aliphatic monocarboxylic acids are known to be inversely linear to the dielectric constants.⁴⁰ Even more important is the fact that lower

analogues of linear alkyl acids tend to exist as multimers, e.g., formic acid trimers⁴¹ and pentamers⁴² were found to be stable according to ab initio calculations. As the alkyl chain length increases, the enhanced hydrophobic effects drive the polar carboxylic acid groups to assemble or aggregate in a less polar fashion so as to minimize electrostatic effects in solution. Indeed, those with longer chain lengths tend to form dimers having zero dipole moment, thus allowing for a stabilization of the carboxylic acid groups in a hydrophobic environment with low dielectric constant.^{43,44}

The general trend of alkanolic acid aggregation in solution may also play a role in the 2D assembly of TMA and BTB on a graphite surface. In the case of BTB, a polarity effect can be applied to rationalize the 2-D structures. In contradiction to TMA, where the flower structure is built up by trimers and the chicken-wire structure by dimers, respectively, the basic unit is now a dimer for both BTB polymorphs. Despite having the dimer dictating the seeding in both cases, the polarity of the solution orchestrates the arrangement of the larger BTB aggregates on the surface, as illustrated by Figure 6. The less polar and less dense chicken-wire structure is generated in the case of the more hydrophobic nonanoic acid, whereas the more polar and denser oblique structure is materialized with the more polar heptanoic acid, as shown in Figure 6. Because the chicken-wire structure exposes a lower number of polar groups, per unit area as well as per number of participating molecules, during the growth, this structure is clearly preferred in a solvent of low dielectric constant and vice versa.

Comparing the different solvents described in Table 1, it seems reasonable to assume a disparate mechanism for the formation of the interfacial monolayer structures depending on whether the solvent can or cannot exert strong hydrogen bonds,

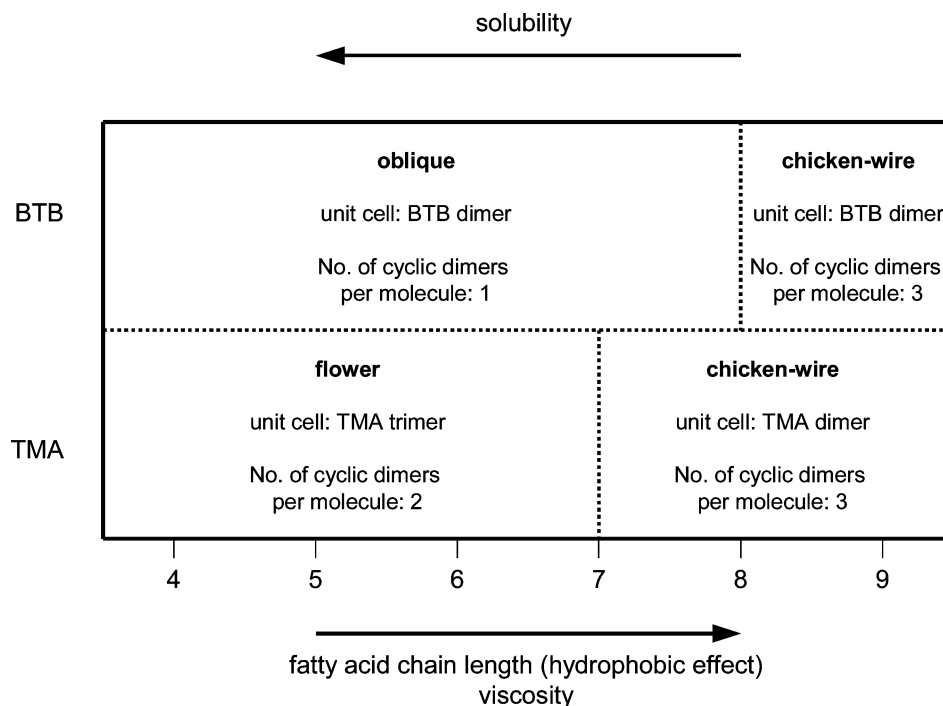


Figure 5. Schematic representation of the properties observed along the homologous series of alkanolic acids from butanoic to nonanoic acid and the respective interfacial monolayer structure.

because the latter is a highly directional intermolecular interaction. In contrast, sizable hydrophobic interactions through van der Waals interactions will require a sufficiently long alkyl chain of the solvent. Thus, it is to be expected that in alkanols and alkanolic acids the interfacial structure will be controlled through hydrogen bonding as long as it is the dominating contribution as compared to hydrophobic contributions, i.e., for shorter and more polar solvents. Indeed, experiments with different hydrogen bonding solvents, altogether three aliphatic alcohols and six fatty acids (see Table 1), reveal a rough dependence of the BTB interfacial monolayer structure on the dielectric constant of the solvent. For $\epsilon = 3, \dots, 10$ the oblique BTB structure is observed exclusively, whereas for $\epsilon \leq 2.5$ the hexagonal BTB structure is preferred. In the intermediate range of $\epsilon = 2.5, \dots, 3$ addressed by testing the homologous series of alkanolic acids, the oblique structure is preferred for $\text{CH}_3(\text{CH}_2)_n\text{COOH}$ with $n = 2, \dots, 5$, whereas coexistence of oblique and hexagonal domains was found in the case of octanoic acid ($n = 6$). With nonanoic acid ($n = 7$) only the hexagonal structure is detected. Unfortunately, there is not a monotonic decrease of ϵ when varying n from 2–7, indicating that in this intermediate range subtle differences in the dielectric constants may be overridden by other effects. Despite these irregularities in the range $3 < \epsilon \leq 2.5$, it seems, however, that there is an overall polarity dependence on the surface structuring for the alkanols and alkanolic acids.

For alkanes and arylalkanes, solvent deviations from the predictions based on the dielectric constant are attributed to the lack of any polar anchor group to induce orientation by hydrogen bonding. For 1-phenyloctane ($\epsilon = 2.26$) the BTB monolayer structure was found to be hexagonal, whereas a mixture of oblique and hexagonal structures was obtained in dodecane ($\epsilon = 2.01$). As stated above, the absence of specific interactions between solvent and solute molecules is expected to lead to a different orienting mechanism as compared to fatty acids and alkanols.

Besides the plausible stabilization of polar units by polar solvents during growth, kinetic effects offer an alternative

explanation for the observed polymorphism. It is reasonable to assume that the adsorption rate (i.e., the number of molecules adsorbing from the liquid on the surface per unit of area and time) of BTB decreases monotonically with increasing solvent chain length. As the length of the aliphatic tail of the solvent molecules increases, the interaction strength between molecules and thus the viscosity of the respective liquid rises. For this reason the diffusion constant of BTB in the respective solvent decreases with increasing chain length of the solvent molecules. Also the solubility of BTB will decrease from heptanoic to nonanoic acid, similar to TMA.³⁴ In general, the longer the chain length of a fatty acid, the more hydrophobic is the liquid. This is because the weight of the carboxylic acid group, also being the responsible functional group for dissolving BTB, diminishes from heptanoic to nonanoic acid. An indication that the structure formation also might be influenced by the adsorption rate was seen in UHV deposition experiments of TMA, where higher deposition rates lead to a preference of the more dense flower structure.⁴⁵ A more dense arrangement would be favored for a higher adsorption rate, because the fast association of the molecules does not allow the system to adopt the structure with the lowest free energy. Also the observed coexistence of both BTB (TMA) polymorphs in octanoic acid and dodecane (heptanoic acid) indicate that kinetics rather than thermodynamics indeed might govern the monolayer structures.

Another explanation is offered by solvent coadsorption; i.e., a particular solvent stabilizes a particular modification by lowering its free energy. Yet, in the STM images a second type of molecule cannot be resolved, we thus exclude incorporation of rather large solvent molecules in neither of the BTB polymorphs. But inclusion of small impurity molecules (e.g., H_2O or other carboxylic acids) cannot be ruled out, especially because the solvents used here exhibit a chemical purity only. In particular, water would be suited for bridging gaps between BTB molecules and might not be resolved in the STM images.

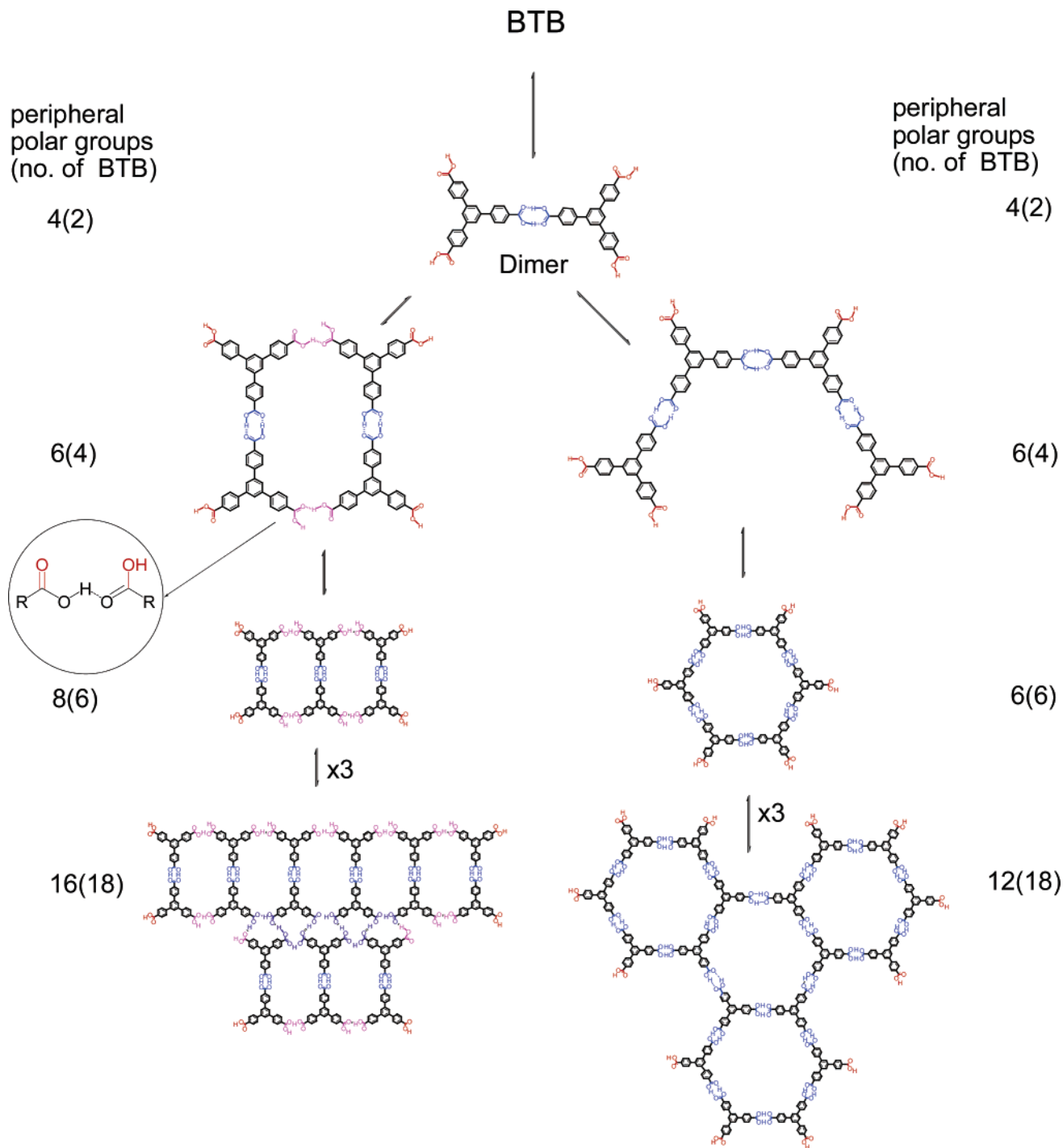


Figure 6. Cartoon of the seeding process on the surface with the BTB dimer as the repeating unit forming the oblique pattern (left) and the chicken wire motif (right). The count represents the number of polar functional groups exposed to the solvent, and those in the brackets represent the number of BTB molecules involved in the assembly. The free polar groups are marked in red and the cyclic dimers of carboxylic acids that have zero dipole effects are marked in blue. The inset circle depicts the catemeric hydrogen-bonding motifs that due to their residual polarity have to be accounted for in the polarity count. Hydrogen bonds interconnecting the dimer rows of the oblique structure are marked violet (saturated bonds) and pink (unsaturated bonds) respectively.

Conclusion

In this work two-dimensional supramolecular host structures were realized by adsorption of BTB molecules on graphite surfaces from the liquid phase. Depending on the solvent used, two different structures with a hexagonal and an oblique unit cell respectively were revealed by means of in situ STM. One of them, the so-called chicken-wire polymorph, exhibits fairly large circular cavities with a diameter of 2.8 nm. Both structures substantially differ in their hydrogen bonding pattern but have

the dimer motif in common. The evolution of different structures for varying solvents is discussed in light of adsorption rates and of stabilization of polar units during the growth. For solvents with functional groups being able to hydrogen bond to the solute, a rough dependence of the structure formation on the dielectric constant was found. The more dense and more polar oblique BTB structure was only observed for solvents with a dielectric constant $\epsilon > 3$. Experiments with other classes of solvents, however, have pointed out that further parameters can be

decisive for the structure formation as well. The subject of ongoing research is the coadsorption of guests such as semi-conducting metal clusters within these cavities, thereby introducing a long-range lateral order of these nanoparticles. Moreover, the spatial fixation of these objects enables further investigations—like scanning tunneling spectroscopy—on isolated objects without the large experimental effort caused by sample cooling.

Acknowledgment. We gratefully acknowledge the DFG for financial support of this work within SFB 486 and DFG Schm 647/13-1.

References and Notes

- (1) Lackinger, M.; Griessl, S.; Markert, T.; Jamitzky, F.; Heckl, W. M. *J. Phys. Chem. B* **2004**, *108*, 13652.
- (2) Stepanow, S.; Strunskus, T.; Lingenfelder, M.; Dmitriev, A.; Spillmann, H.; Lin, N.; Barth, J. V.; Woll, C.; Kern, K. *J. Phys. Chem. B* **2004**, *108*, 19392.
- (3) Yokoyama, T.; Yokoyama, S.; Kamikado, T.; Okuno, Y.; Mashiko, S. *Nature* **2001**, *413*, 619.
- (4) Rosei, F.; Schunack, M.; Jiang, P.; Gourdon, A.; Laegsgaard, E.; Stensgaard, I.; Joachim, C.; Besenbacher, F. *Science* **2002**, *296*, 328.
- (5) Schunack, M.; Petersen, L.; Kuhnle, A.; Laegsgaard, E.; Stensgaard, I.; Johannsen, I.; Besenbacher, F. *Phys. Rev. Lett.* **2001**, *86*, 456.
- (6) Glass, R.; Moller, M.; Spatz, J. P. *Nanotechnology* **2003**, *14*, 1153.
- (7) Shchukin, V. A.; Ledentsov, N. N.; Bimberg, D. *Physica E* **2001**, *9*, 140.
- (8) Gerardot, B. D.; Subramanian, G.; Minvielle, S.; Lee, H.; Johnson, J. A.; Schoenfeld, W. V.; Pine, D.; Speck, J. S.; Petroff, P. M. *J. Cryst. Growth* **2002**, *236*, 647.
- (9) Gimzewski, J. K.; Joachim, C.; Schlittler, R. R.; Langlais, V.; Tang, H.; Johannsen, I. *Science* **1998**, *281*, 531.
- (10) Mayor, M.; Buschel, M.; Fromm, K. M.; Lehn, J. M.; Daub, J. *Chem. Eur. J.* **2001**, *7*, 1266.
- (11) Griessl, S.; Lackinger, M.; Edelwirth, M.; Hietschold, M.; Heckl, W. M. *Single Mol.* **2002**, *3*, 25.
- (12) Dmitriev, A.; Lin, N.; Weckesser, J.; Barth, J. V.; Kern, K. *J. Phys. Chem. B* **2002**, *106*, 6907.
- (13) Ishikawa, Y.; Ohira, A.; Sakata, M.; Hirayama, C.; Kunitake, M. *Chem. Commun.* **2002**, 2652.
- (14) Su, G. J.; Zhang, H. M.; Wan, L. J.; Bai, C. L.; Wandlowski, T. *J. Phys. Chem. B* **2004**, *108*, 1931.
- (15) Han, B.; Li, Z.; Pronkin, S.; Wandlowski, T. *Can. J. Chem.* **2004**, *82*, 1481.
- (16) Lu, J.; Zeng, Q. D.; Wang, C.; Zheng, Q. Y.; Wan, L. J.; Bai, C. L. *J. Mater. Chem.* **2002**, *12*, 2856.
- (17) Theobald, J. A.; Oxtoby, N. S.; Phillips, M. A.; Champness, N. R.; Beton, P. H. *Nature* **2003**, *424*, 1029.
- (18) Kampschulte, L.; Griessl, S.; Heckl, W. M.; Lackinger, M. *J. Phys. Chem. B* **2005**, *109*, 14074.
- (19) Stepanow, S.; Lingenfelder, M.; Dmitriev, A.; Spillmann, H.; Delvigne, E.; Lin, N.; Deng, X. B.; Cai, C. Z.; Barth, J. V.; Kern, K. *Nat. Mater.* **2004**, *3*, 229.
- (20) Griessl, S. J. H.; Lackinger, M.; Jamitzky, F.; Markert, T.; Hietschold, M.; Heckl, W. M. *J. Phys. Chem. B* **2004**, *108*, 11556.
- (21) Griessl, S. J. H.; Lackinger, M.; Jamitzky, F.; Markert, T.; Hietschold, M.; Heckl, W. A. *Langmuir* **2004**, *20*, 9403.
- (22) Lu, J.; Lei, S. B.; Zeng, Q. D.; Kang, S. Z.; Wang, C.; Wan, L. J.; Bai, C. L. *J. Phys. Chem. B* **2004**, *108*, 5161.
- (23) Chae, H. K.; Siberio-Perez, D. Y.; Kim, J.; Go, Y.; Eddaoudi, M.; Matzger, A. J.; O'Keeffe, M.; Yaghi, O. M. *Nature* **2004**, *427*, 523.
- (24) Kitaigorodskii, A. I. *Organic Chemical Crystallography*; Consultants Bureau: New York, 1959.
- (25) Kitaigorodskii, A. I. *Acta Crystallogr.* **1965**, *18*, 585.
- (26) Yan, H. J.; Lu, J.; Wan, L. J.; Bai, C. L. *J. Phys. Chem. B* **2004**, *108*, 11251.
- (27) Weber, E.; Hecker, M.; Koeppe, E.; Orlia, W.; Czugler, M.; Csoregh, I. *J. Chem. Soc., Perkin Trans. 2* **1988**, 1251.
- (28) Gyarfás, B. J.; Wiggins, B.; Zosel, M.; Hipps, K. W. *Langmuir* **2005**, *21*, 919.
- (29) Desiraju, G. R. *Acc. Chem. Res.* **1996**, *29*, 441.
- (30) Neuheuser, T.; Hess, B. A.; Reutel, C.; Weber, E. *J. Phys. Chem.* **1994**, *98*, 6459.
- (31) Kuduva, S. S.; Craig, D. C.; Nangia, A.; Desiraju, G. R. *J. Am. Chem. Soc.* **1999**, *121*, 1936.
- (32) Berkovitch-Yellin, Z.; Leiserowitz, L. *J. Am. Chem. Soc.* **1982**, *104*, 4052.
- (33) Kolotuchin, S. V.; Thiessen, P. A.; Fenlon, E. E.; Wilson, S. R.; Loweth, C. J.; Zimmerman, S. C. *Chem. Eur. J.* **1999**, *5*, 2537.
- (34) Lackinger, M.; Griessl, S.; Heckl, W. A.; Hietschold, M.; Flynn, G. W. *Langmuir* **2005**, *21*, 4984.
- (35) Lei, S. B.; Wang, C.; Yin, S. X.; Wang, H. N.; Xi, F.; Liu, H. W.; Xu, B.; Wan, L. J.; Bai, C. L. *J. Phys. Chem. B* **2001**, *105*, 10838.
- (36) Wohlfarth, C. *Static Dielectric Constants of Pure Liquids and Binary Liquid Mixtures, Macroscopic and Technical Properties of Matter*; Vol. 6 Numerical Data and Functional Relationships in Science and Technology; Springer-Verlag: Berlin, Heidelberg, New York, 1991.
- (37) *Landolt-Börnstein*. 1991; Vol. 6.
- (38) Fisher, C. H. *J. Am. Oil Chem. Soc.* **1988**, *65*, 1647.
- (39) Shanmugasundaram, V.; Thiagarajan, P. *J. Indian Chem. Soc.* **1986**, *63*, 589.
- (40) Conti, F.; Franconi, C. *Ber. Bunsen-Ges. Phys. Chem.* **1967**, *71*, 146.
- (41) Roy, A. K.; Thakkar, A. J. *Chem. Phys. Lett.* **2004**, *386*, 162.
- (42) Roy, A. K.; Thakkar, A. J. *Chem. Phys.* **2005**, *312*, 119.
- (43) Loveluck, G. *J. Phys. Chem.* **1960**, *64*, 385.
- (44) Mognaschi, E. R.; Zullino, L.; Chierico, A. *J. Phys. D-Appl. Phys.* **1984**, *17*, 1007.
- (45) Griessl, S.; Lackinger, M. Unpublished observation.